



HHS Public Access

Author manuscript

Immunobiology. Author manuscript; available in PMC 2017 March 01.

Published in final edited form as:

Immunobiology. 2016 March ; 221(3): 468–474. doi:10.1016/j.imbio.2015.11.003.

Mast cells and histamine alter intestinal permeability during malaria parasite infection

Rashaun A. Potts, Caitlin M. Tiffany, Nazzy Pakpour, Kristen L. Lokken, Connor R. Tiffany, Kong Cheung, Renée M. Tsois, and Shirley Luckhart*

Department of Medical Microbiology and Immunology, School of Medicine, University of California, Davis, Davis, CA 95616

Rashaun A. Potts: rapotts@ucdavis.edu; Caitlin M. Tiffany: cmtiffany@ucdavis.edu; Nazzy Pakpour: npakpour@ucdavis.edu; Kristen L. Lokken: kllokken@ucdavis.edu; Connor R. Tiffany: crtiffany@ucdavis.edu; Kong Cheung: kcheung@ucdavis.edu; Renée M. Tsois: rmtsolis@ucdavis.edu

Abstract

Co-infections with malaria and non-typhoidal *Salmonella* serotypes (NTS) can present as life-threatening bacteremia, in contrast to self-resolving NTS diarrhea in healthy individuals. In previous work with our mouse model of malaria/NTS co-infection, we showed increased gut mastocytosis and increased ileal and plasma histamine levels that were temporally associated with increased gut permeability and bacterial translocation. Here, we report that gut mastocytosis and elevated plasma histamine are also associated with malaria in an animal model of falciparum malaria, suggesting a broader host distribution of this biology. In support of mast cell function in this phenotype, malaria/NTS co-infection in mast cell-deficient mice was associated with a reduction in gut permeability and bacteremia. Further, antihistamine treatment reduced bacterial translocation and gut permeability in mice with malaria, suggesting a contribution of mast cell-derived histamine to GI pathology and enhanced risk of bacteremia during malaria/NTS co-infection.

Keywords

mast cell; histamine; co-infection; bacteremia; malaria; *Plasmodium*; *Salmonella*

1. Introduction

Nearly half of the global population is at risk for malaria, which results in approximately 600,000 deaths annually (WHO, 2014). Most of these deaths are due to *Plasmodium falciparum* infection in sub-Saharan Africa in pediatric patients, a population with a high

*Corresponding author: 3437 Tupper Hall, One Shields Avenue, Department of Medical Microbiology and Immunology, School of Medicine, University of California, Davis, Davis, CA 95616 USA, TEL: +1 530 754 6963, FAX: +1 530 752 8692, sluckhart@ucdavis.edu.

Conflict of Interest

The authors declare no conflicts of interest.

Publisher's Disclaimer: This is a PDF file of an unedited manuscript that has been accepted for publication. As a service to our customers we are providing this early version of the manuscript. The manuscript will undergo copyediting, typesetting, and review of the resulting proof before it is published in its final citable form. Please note that during the production process errors may be discovered which could affect the content, and all legal disclaimers that apply to the journal pertain.

prevalence of co-infection with non-typhoidal serotypes of *Salmonella* (NTS) (Reddy et al., 2015). In healthy individuals, infections with NTS are associated with gastroenteritis, a localized infection with low mortality. However, co-infected individuals can develop a life-threatening NTS bacteremia (Scott et al., 2015) that is complicated by the increasing prevalence of antibiotic resistance in Africa (Feasey et al., 2015; Kingsley et al., 2009).

In the course of infection, sequestration of parasitized red blood cells (RBCs) causes capillary blockage that is prominent in intestinal villi (Seydel et al., 2006) and associated with increased gastrointestinal (GI) permeability (Molyneux et al., 1989; Wilairatana et al., 1997). Severe malaria has also been associated with high circulating histamine (Enwonwu et al., 2000; Srichaikul et al., 1976), suggesting a connection between allergic inflammation and disease. To identify mechanisms behind increased GI permeability, invasive bacterial disease, and bacteremia during malaria infection, we developed a murine model of co-infection with *Plasmodium yoelii* and the NTS strain *Salmonella enterica* serotype Typhimurium (Roux et al., 2010). In this model, co-infected mice have higher levels of *S. Typhimurium* in their mesenteric lymph nodes, spleens, and livers than do mice infected with *S. Typhimurium* alone (Roux et al., 2010). Further, we observed that rising parasitemia is associated with increased intestinal permeability, increased circulating and ileal histamine levels, and ileal mastocytosis, suggesting that allergic inflammation contributes to GI pathology in our mouse co-infection model (Chau et al., 2013).

Mucosal mast cells are primary regulators of the physical integrity and function of the intestinal epithelial barrier (Gurish and Austen, 2012).. In the context of parasitic infections, intestinal mastocytosis is required for expulsion of GI nematodes, via intestinal permeability that is enhanced by mast cell protease-dependent alterations to intercellular tight junctions and adherens junctions (Grencis et al., 2014). In this context, mast cells are recruited and traffic from the submucosa to the villus tips, returning to the crypts once infection is resolved (Friend et al., 1998). Other mast cell-derived mediators, however, have been associated with secretory diarrhea and intestinal malabsorption, including histamine (Castro et al., 1987; Madden et al., 2002). This is particularly notable in mastocytic enterocolitis, chronic intestinal permeability that is reversible by treatment with H1 and H2 histamine receptor antagonists (Jakate et al., 2006).

Based on our observations of increased ileal mastocytosis and histamine in our mouse malaria model and related facts regarding mastocytosis and other parasitic infections, we asked whether mastocytosis and elevated circulating histamine levels were more broadly evident in malaria using a non-human primate model of falciparum malaria and whether mast cell ablation and antihistamine therapy in in our mouse model could increase the integrity and function of the intestinal epithelial barrier, thereby reducing bacterial translocation during *S. Typhimurium* co-infection.

2. Materials and methods

2.1. Animals

Control uninfected and *Plasmodium fragile*-infected Rhesus macaque (*Macaca mulatta*) tissues were from two previous studies (Mooney et al., 2014; Raffatellu et al., 2008). Six- to

8-week-old female CBA/J mice and WBB6F1/J-*Kit*^W/*Kit*^{W-v} mice and their wild type littermate controls were purchased from Jackson West. Female CD-1 mice for parasite stock expansion were from Harlan. Macaque and mouse protocols were reviewed and deemed to be in accord with all relevant institutional policies and federal guidelines by the University of California Davis Institutional Animal Care and Use Committee.

2.2. Parasites and bacteria

Mice were inoculated intraperitoneally (i.p.) on day 0 with 0.1 ml of uninfected CD-1 RBCs (uninfected control) or with 10⁷ *P. yoelii* 17XNL-infected RBCs. Mice were orally gavaged at 9 days after RBC inoculation with 20 mg of streptomycin to enhance subsequent colonization (at 10 days after RBC inoculation) of *E. coli* Nissle, which is resistant to streptomycin and ampicillin, or *S. Typhimurium* strain IR715 (pHP45Ω), which is resistant to streptomycin, ampicillin, and nalidixic acid (Supplementary Fig. 1). For both bacterial species, mice were inoculated with 0.1 ml of an overnight culture (37°C) of 10⁸ colony-forming units (CFU) following our previous protocol (Chau et al., 2013).

2.3. Microbial readouts for mouse infection

Parasitemias were recorded beginning 2 days following infection with *P. yoelii* 17XNL (hereafter, *P. yoelii*) as infected RBCs divided by the total number of RBCs in Giemsa-stained thin blood films. To quantify tissue *S. Typhimurium* CFU, liver and spleen were aseptically removed and homogenized in cold phosphate-buffered saline (PBS) using an Ultra Turrax T25 basic mixer (IKA Works, Inc., Wilmington, NC). Serial dilutions were plated on selective media (LB agar plus ampicillin or LB agar plus nalidixic acid; Sigma-Aldrich, St. Louis, MO) and grown overnight at 37°C. To quantify blood CFU, blood was collected from the heart via heparinized needle, plasma removed, then incubated for 10 min in 1% Triton X-100. Samples were serially diluted and plated on LB agar plates containing 100mg/L nalidixic acid. After overnight growth at 37°C, CFU/gram of tissue and blood were calculated. To quantify bacterial DNA in mouse spleen, DNA was extracted using DNeasy Blood & Tissue kit (Qiagen, Valencia, CA) from tissue treated with enzymatic lysis buffer to release bacterial DNA according to manufacturer's instructions. Quantitative real-time PCR (qPCR) was performed using eubacterial 16S ribosomal DNA primers 5'-ACTCCTACGGGAGGCAGCAGT-3', and 5'-ATTACCGCGGCTGCTGGC-3', SYBR green and ViiA 7 Real-Time PCR System (Applied Biosystems, Grand Island, NY). Plasmid standards were included in each run for absolute quantification.

2.4. Mast cell tryptase immunofluorescence of Rhesus macaque ileum sections

Paraffin embedded ileal sections were deparaffinized and hydrated. Antigen retrieval was completed in 10mM sodium citrate buffer, pH 6.0 at a sub-boiling temperature for 10 minutes. Endogenous peroxidase activity was quenched with 3% H₂O₂ in dH₂O for 10 minutes. Non-specific binding was blocked with 5% goat serum in 1X Tris Buffered saline, 0.1% Tween-20 (Sigma-Aldrich; TBST) for 1 hour at room temperature. Sections were incubated overnight at 4 C with a 1:500 dilution of mouse anti-human mast cell tryptase antibody, AA1 (Santa Cruz Biotechnology, Inc., Santa Cruz, CA) or with PBS as a negative control. After three washes in TBST, sections were incubated with a 1:3000 dilution of goat

anti-mouse IgG-HRP (Santa Cruz Biotechnology) for 1 hour at room temperature, washed, and reacted with diaminobenzidine (DAB) chromagen substrate (Cell Signaling Technology, Inc., Danvers, MA). Sections were counterstained with hematoxylin, dehydrated in alcohol, cleared in xylene, and mounted in Cytoseal 60 (Thermoscientific, Pittsburgh, PA). For each animal examined, mast cells were identified for an average of six ileal sections in 10 different fields using a Nikon Eclipse E800 microscope at 20× magnification.

2.5. E-cadherin immunofluorescence of mouse ileum sections

Sections were stained for E-cadherin as described (Chau et al., 2013) and viewed using a FluoView FV1000 confocal microscope (Olympus, Center Valley, PA) with a 40× objective. ImageJ software was used to analyze five fields per slide for three slides per group of mice.

2.6. Quantification of Rhesus macaque plasma histamine

Plasma histamine levels were determined by enzyme immunoassay (Oxford Biomedical Research, Rochester Hills, MN) per the manufacturer's instructions.

2.7. Antihistamine treatment of mice

P. yoelii infected CBA/J mice were injected i.p. with 40 mg/kg pyrilamine (H1 receptor antagonist) or saline (vehicle control) daily from days 1–8 after infection.

2.8. qPCR for mouse ileal and splenic cytokine transcripts

Tissue RNAs were extracted using TRIzol reagent (Invitrogen) and cDNAs were synthesized using QuantiTect reverse transcription kit (Qiagen) according to the manufacturers' instructions. cDNA samples were preamplified using Advantage 2 DNA polymerase mix (Clontech, Mountain View, CA). qPCR was performed using Gene Expression Assays for mouse *interleukin (il) 4*, *il6*, *il10*, *tumor necrosis factor alpha (tnfa)*, *interferon gamma (ifng)* (Applied Biosystems; efficiency 91%), and *beta-2-microglobulin (b2m)*; (Applied Biosystems; efficiency 93.6%) using a 7900HT fast real-time PCR instrument (Applied Biosystems). Samples were analyzed in triplicate to confirm uniform amplification using recommended cycling conditions. Treatment cytokine transcript levels were normalized against *b2m* levels using the comparative threshold cycle (C_T) method and are represented as fold changes over control levels.

2.9. Lactulose-mannitol assay for intestinal permeability

WBB6F1/J-*Kit^W/Kit^{W-v}* mice were co-infected with *P. yoelii* and *S. Typhimurium* as described above. At 1, 3, 5, 7, 9, and 11 days after parasite infection, mice were gavaged with lactulose and mannitol solutions and urine was collected and analyzed as described (Chau et al., 2013).

2.10. Statistical analysis

All data were analyzed for normality using GraphPad InStat 5.0 (GraphPad Software Inc., La Jolla, CA). Parasitemia data were analyzed using unpaired *t*-test on daily measurements; lactulose:mannitol ratio data and CFU data were analyzed using Student's *t*-test or Mann-

Whitney *U* test ($\alpha=0.05$). Real-time PCR data were transformed prior to ANOVA and Student-Neuman-Keuls means separation ($\alpha=0.10$).

3. Results

3.1. *P. fragile*-infected Rhesus macaques exhibit increased ileal mastocytosis and plasma histamine levels

Rhesus macaques infected with *P. fragile* model key aspects of *P. falciparum* infection, including non-relapsing infection, parasite sequestration, and cerebral malaria (Fujioka et al., 1994). We used previously collected tissue and plasma to determine whether ileal mastocytosis and elevated circulating histamine levels were evident in this model. As reported, animals developed maximal parasitemias at 10–12 days post infection (PI), which declined in 3 of 4 animals after sub-curative treatment (Mooney et al., 2014). Peak parasitemias were 1–4% in three animals and 0.4% in the fourth animal (Supplementary Fig. 2A). Ileal sections from *P. fragile*-infected animals (14–15 days PI) showed mast cells in the submucosa and villi, whereas no mast cells were detected in ileal tissue of healthy controls (Fig. 1A). Plasma histamine levels were maximal prior to peak parasitemia and declined with falling parasitemia in two of three animals (283, 103) for which samples were available through 15 days (Fig. 1B, Supplementary Fig. 2B).

3.2. Co-infected mast cell deficient mice exhibit decreased intestinal permeability

To assess the contribution of mast cells to malaria-induced changes to the intestine, we used mast cell-deficient WBB6F1/J-*Kit*^W/*Kit*^{W-v} mice, which possess a single base substitution in *c-kit*, are completely deficient of mast cells, and have 5–10% of whole body histamine levels of matched wild type mice (Yamatodani et al., 1982). Despite reported anemia, blood and bone marrow neutrophil functional responses of *Kit*^W/*Kit*^{W-v} mice are indistinguishable from wild type mice (Chervenick, 1969). In *Kit*^W/*Kit*^{W-v} mice and their wild type controls, *P. yoelii* parasitemias were indistinguishable after 3 days PI (Fig. 2A). However, GI permeability as measured by lactulose:mannitol ratio was significantly decreased in mast cell-deficient mice at 1 day post parasite infection (Fig. 2B) and trended toward decreased permeability through 12 days PI/2 days post co-infection (not shown) when animals were sacrificed to assess tissue cytokine levels, *S. Typhimurium* CFU, and E-cadherin staining in the ileum.

IL-4 is produced by activated mast cells and we previously observed significantly higher levels of ileal *il4* in *P. yoelii*-infected CBA/J mice relative to uninfected controls (Chau et al., 2013). In *Kit*^W/*Kit*^{W-v} co-infected mice, in contrast, *il4* transcript levels in spleen and liver were not reduced, but rather were increased, although not significantly relative to levels in wild type matched controls (Figs. 2C, D). Further, inflammatory (*il6*, *tnfa*, *ifng*) and anti-inflammatory (*il10*) cytokine transcript levels trended lower in tissues from mast cell-deficient mice relative to co-infected wild type controls (Figs. 2C, D). Despite reduced inflammatory cytokine transcript levels (Figs. 2C, D), co-infected mast cell-deficient mice trended toward decreased *S. Typhimurium* CFU in the spleen and liver and exhibited significantly reduced blood CFU, a relevant proxy for bacteremia, at 2 days after bacterial co-infection (Fig. 2E). While decreased bacteremia in the absence of mast cells could result

in part from better control over multiplication of disseminated bacteria, differences at this early time point after infection suggested enhanced control of bacterial dissemination from the intestinal tract.

Intestinal homeostasis is maintained by localized immune responses and epithelial junction integrity (Peterson and Artis, 2014), suggesting that in the absence of enhanced immunity, enhanced junction integrity in mast cell-deficient mice could account for reduced bacterial translocation in co-infection. In support, E-cadherin staining in the ileum of co-infected mast cell-deficient mice was dramatically enhanced relative to that in co-infected wild type controls (Fig. 2F) and the opposite of reduced E-cadherin staining during malaria-induced mastocytosis in CBA/J mice (Chau et al., 2013).

3.3. Antihistamine treatment during *Plasmodium yoelii* infection results in decreased intestinal permeability

Mast cell-derived histamine can rapidly reduce E-cadherin adhesion and transepithelial resistance (Zabner et al., 2003) to diminish barrier integrity (Wang et al., 1995) and, in this context, pyrilamine has been shown to block mast cell-dependent effects of histamine in the mouse intestine (Coleman, 2002). Accordingly, we used pyrilamine to assess the contribution of histamine to malaria-induced changes in the mouse intestine. CBA/J mice were infected with *P. yoelii* and treated with pyrilamine or saline (vehicle control) from days 1–8 PI, the period of elevated ileal histamine in our previous studies (Chau et al., 2013). At 10 days PI, mice were colonized with non-invasive, non-pathogenic *E. coli* Nissle (EcN) for an independent assessment of GI permeability and for direct comparison with previous studies (Chau et al., 2013). Further, since EcN was originally isolated as an intestinal commensal, any bacteria that spread from the intestine should be unable to replicate systemically, therefore any effect of histamine on bacterial translocation from the gut would be a direct effect of changes in intestinal permeability, rather than replication of bacteria at systemic sites. Mice were sacrificed at 14 days PI *P. yoelii*/4 days post-colonization to quantify eubacterial 16S rDNA levels in the spleen as a measure for translocating intestinal microbiota. Uninfected controls were colonized with EcN for an identical period (4 days). Interestingly, the pyrilamine treated group had significantly higher parasitemia at 8–11 days PI (Fig. 3A). This enhanced parasitemia contrasts with findings for oral antihistamine treatment during *P. yoelii nigeriensis* infection of Swiss mice and with i.p. antihistamine treatment and genetic ablation of histidine decarboxylase (HDC) during *Plasmodium berghei* (NK65 and ANKA) infection of C57BL/6 mice. In particular, these studies showed that antihistamine treatment and HDC deficiency had no effect or a negative effect on parasitemia (Singh and Puri, 1998; Beghdadi et al., 2008). Although observed pyrilamine enhancement of parasitemia could derive in part from experimental differences (*P. yoelii* 17XNL, CBA/J mice, EcN colonization), these mice importantly trended toward *reduced* bacterial translocation, with a 40% reduction in splenic 16S rDNA copies relative to saline treatment at 14 days PI *P. yoelii*/4 days post colonization (Fig. 3B). Consistent with this, E-cadherin staining in pyrilamine-treated *P. yoelii*-infected mice was more intense than in saline-treated infected mice and indistinguishable from that of uninfected mice (Fig. 3C). Accordingly, our data demonstrate that intestinal permeability was enhanced by histamine-

associated changes to the intestinal epithelial barrier that were independent of a 2–3% difference in parasitemia.

4. Discussion

Previous work in our lab suggested that malaria-associated hypoargininemia and low nitric oxide (NO) availability induce recruitment of mast cells to the mouse ileum (Chau et al., 2013). Mast cells can be activated under conditions of low NO (Abraham and St. John, 2010) and are critical effector cells in immediate-type allergic reactions via the release of enzymes, cytokines, and histamine (Abraham and St. John, 2010). Reversal of mastocytosis by increasing bioavailable L-Arginine reduced bacterial translocation in *P. yoelii*-infected mice (Chau et al., 2013), suggesting that mast cells were functionally involved in increased intestinal permeability.

Our findings here confirm that ileal mastocytosis and elevated histamine in malaria are not unique to mice and contribute to infection-associated GI permeability (Fig. 4). In particular, the absence of mast cells in our mouse co-infection model reduced GI permeability, bacterial translocation and, importantly, bacteria in the blood independently of effects on malaria parasite infection. Further, our observations of ileal mastocytosis in a non-human primate model suggest that mast cells may be cause-and-effect with GI permeability in human malaria. Antihistamine therapy showed a trend toward reduced GI permeability and bacterial translocation in the mouse, suggesting that other mast cell-derived factors likely contribute to GI permeability to resident microbiota, bacterial pathogens, and perhaps ligands such as lipopolysaccharide or peptidoglycan in malaria (Olupot-Olupot et al., 2013).

In conclusion, mast cells are protective during GI parasite infections, inducing an allergic response via the actions of histamine and other effectors that can alter GI homeostasis (Grencis et al., 2014). Interestingly, cytokine levels were not consistent with a protective immune response in the intestine of mast cell-deficient mice (Fig. 2C), suggesting that inflammatory cytokines of the immunological barrier may not be the ideal target for reducing bacterial translocation in pediatric patients. Instead, reducing the effects of mast cell-derived histamine and enhancing the physical barrier through L-Arginine supplementation to reduce mastocytosis may yield more promising results. Further studies will be needed to determine if these mechanisms occur in the pediatric malaria population and if reducing mast cell activation and the effects of mast cell-derived factors can decrease clinical risk of invasive bacterial infection.

Supplementary Material

Refer to Web version on PubMed Central for supplementary material.

Acknowledgments

We are grateful for guidance for mast cell tryptase staining from the laboratory of Dr. George H. Caughey (San Francisco Veteran's Administration Medical Center and University of California, San Francisco). This work was supported with funds provided by the University of California Davis and by NIH NIAID R01 AI098078.

Abbreviations

NTS	non-typhoidal <i>Salmonella</i> serotypes
GI	gastrointestinal
RBC	red blood cell
H1	histamine receptor 1
H2	histamine receptor 2
i.p	intraperitoneally
CFU	colony forming units
PBS	phosphate-buffered saline
LB	Luria-Bertani medium
TBST	Tris-buffered Saline
IL	interleukin (IL-10, 4, 6)
TNFα	tumor necrosis factor alpha
IFNγ	interferon gamma
B2M	beta-2-microglobulin
EcN	<i>Escherichia coli</i> Nissle
NO	nitric oxide

References

- Abraham SN, St John AL. Mast cell-orchestrated immunity to pathogens. *Nat Rev Immunol.* 2010; 10:440–452.10.1038/nri2782 [PubMed: 20498670]
- Beghdadi W, Porcherie A, Schneider BS, Dubayle D, Peronet R, Huerre M, Watanabe T, Ohtsu H, Louis J, Mécheri S. Inhibition of histamine-mediated signaling confers significant protection against severe malaria in mouse models of disease. *J Exp Med.* 2008; 205:395–408.10.1084/jem.20071548 [PubMed: 18227221]
- Castro GA, Harari Y, Russell D. Mediators of anaphylaxis-induced ion transport changes in small intestine. *Am J Physiol - Gastrointest Liver Physiol.* 1987; 253:G540–G548.
- Chau JY, Tiffany CM, Nimishakavi S, Lawrence Ja, Pakpour N, Mooney JP, Lokken KL, Caughey GH, Tsolis RM, Luckhart S. Malaria-associated L-Arginine deficiency induces mast cell-associated disruption to intestinal barrier defenses against non-typhoidal *Salmonella* bacteremia. *Infect Immun.* 2013; 81:3515–3526.10.1128/IAI.00380-13 [PubMed: 23690397]
- Chervenick PABD. Decreased neutrophils and megakaryocytes in anemic mice of genotype W/W. *J Cell Physiol.* 1969; 73:25–30. [PubMed: 5765776]
- Coleman JW. Nitric oxide: a regulator of mast cell activation and mast cell-mediated inflammation. *Clin Exp Immunol.* 2002; 129:4–10. [PubMed: 12100016]
- Dy M, Schneider E. Histamine-cytokine connection in immunity and hematopoiesis. *Cytokine Growth Factor Rev.* 2004; 15:393–410. [PubMed: 15450254]
- Enwonwu CO, Afolabi BM, Salako LO, Idigbe EO, Bashirelahi N. Increased plasma levels of histidine and histamine in falciparum malaria: relevance to severity of infection. *J Neural Transm.* 2000; 107:1273–1287.10.1007/s007020070017 [PubMed: 11145003]

- Friend DS, Ghildyal N, Gurish MF, Hunt J, Hu X, Austen KF, Stevens RL. Reversible Expression of Tryptases and Chymases in the Jejunal Mast Cells of Mice Infected with *Trichinella spiralis*. *J Immunol*. 1998; 160:5537–5545. [PubMed: 9605158]
- Fujioka H, Millet P, Maeno Y, Nakazawa S, Ito Y, Howard RJ, Collins WE, Aikawa M. A Nonhuman Primate Model for Human Cerebral Malaria: Rhesus-Monkeys Experimentally Infected with *Plasmodium fragile*. *Exp Parasitol*. 1994; 78:371–376. <http://dx.doi.org/10.1006/expr.1994.1040>. [PubMed: 7515825]
- Grencis RK, Humphreys NE, Bancroft AJ. Immunity to gastrointestinal nematodes: mechanisms and myths. *Immunol Rev*. 2014; 260:183–205.10.1111/imr.12188 [PubMed: 24942690]
- Gurish MF, Austen KF. Developmental origin and functional specialization of mast cell subsets. *Immunity*. 2012; 37:25–33.10.1016/j.immuni.2012.07.003 [PubMed: 22840841]
- Jakate S, Demeo M, John R, Tobin M, Keshavarzian A. Mastocytic enterocolitis: increased mucosal mast cells in chronic intractable diarrhea. *Arch Pathol Lab Med*. 2006; 130:362–367.10.1043/1543-2165(2006)130[362:MEIMMC]2.0.CO;2 [PubMed: 16519565]
- Lokken KL, Mooney JP, Butler BP, Xavier MN, Chau JY, Schaltenberg N, Begum RH, Müller W, Luckhart S, Tsolis RM. Malaria parasite infection compromises control of concurrent systemic non-typhoidal *Salmonella* infection via IL-10-mediated alteration of myeloid cell function. *PLoS Pathog*. 2014; 10:e1004049.10.1371/journal.ppat.1004049 [PubMed: 24787713]
- Madden KB, Whitman L, Sullivan C, Gause WC, Urban JF, Katona IM, Finkelman FD, Shea-Donohue T. Role of STAT6 and mast cells in IL-4- and IL-13-induced alterations in murine intestinal epithelial cell function. *J Immunol*. 2002; 169:4417–4422.10.4049/jimmunol.169.8.4417 [PubMed: 12370375]
- Molyneux ME, Looareesuwan S, Menzies IANS, Grainger SU, Phillips RE, Warrell DA. Reduced hepatic blood flow and intestinal malabsorption in severe falciparum malaria. 1989; 40:470–476.
- Mooney JP, Butler BP, Lokken KL, Xavier MN, Chau JY, Schaltenberg N, Dandekar S, George MD, Santos RL, Luckhart S, Tsolis RM. The mucosal inflammatory response to non-typhoidal *Salmonella* in the intestine is blunted by IL-10 during concurrent malaria parasite infection. *Mucosal Immunol*. 2014; 7:1302–1311. [PubMed: 24670425]
- Olupot-Olupot P, Urban BC, Jemutai J, Nteziyaremye J, Fanjo HM, Karanja H, Karisa J, Ongodia P, Bwonyo P, Gitau EN, Talbert A, Akech S, Maitland K. Endotoxaemia is common in children with *Plasmodium falciparum* malaria. *BMC Infect Dis*. 2013; 13:117.10.1186/1471-2334-13-117 [PubMed: 23497104]
- Peterson LW, Artis D. Intestinal epithelial cells: regulators of barrier function and immune homeostasis. *Nat Rev Immunol*. 2014; 14:141–153. [PubMed: 24566914]
- Raffatelli M, Santos RL, Verhoeven DE, George MD, Wilson RP, Winter SE, Godinez I, Sankaran S, Paixao TA, Gordon MA, Kolls JK, Dandekar S, Bäumlner AJ. Simian immunodeficiency virus-induced mucosal interleukin-17 deficiency promotes *Salmonella* dissemination from the gut. *Nat Med*. 2008; 14:421–428.10.1038/nm1743 [PubMed: 18376406]
- Reddy EA, Shaw AV, Crump JA. Community-acquired bloodstream infections in Africa: a systematic review and meta-analysis. *Lancet Infect Dis*. 2015; 10:417–432.10.1016/S1473-3099(10)70072-4 [PubMed: 20510282]
- Roux CM, Butler BP, Chau JY, Paixao TA, Cheung KW, Santos RL, Luckhart S, Tsolis RM. Both hemolytic anemia and malaria parasite-specific factors increase susceptibility to nontyphoidal *Salmonella enterica* serovar Typhimurium infection in mice. *Infect Immun*. 2010; 78:1520–1527.10.1128/IAI.00887-09 [PubMed: 20100860]
- Scott JAG, Berkley JA, Mwangi I, Ochola L, Uyoga S, Macharia A, Ndila C, Lowe BS, Mwarumba S, Bauni E, Marsh K, Williams TN. Relation between falciparum malaria and bacteraemia in Kenyan children: a population-based, case-control study and a longitudinal study. *Lancet*. 2015; 378:1316–1323.10.1016/S0140-6736(15)00888-X [PubMed: 21903251]
- Seydel KB, Milner DA, Kamiza SB, Molyneux ME, Taylor TE. The distribution and intensity of parasite sequestration in comatose Malawian children. *J Infect Dis*. 2006; 194:208–215.10.1086/505078 [PubMed: 16779727]
- Singh N, Puri SK. Causal prophylactic activity of antihistaminic agents against *Plasmodium yoelii* nigeriensis infection in Swiss mice. *Acta Trop*. 1998; 69:255–260. [PubMed: 9638277]

- Srichaikul T, Archararit N, Siriasawakul TVT. Histamine changes in *Plasmodium falciparum* malaria. *Trans R Soc Trop Med Hyg.* 1976; 70:36–38. [PubMed: 772896]
- Wang L, Stanisz AM, Wershil BK, Galli SJ, Perdue MH. Substance P induces ion secretion in mouse small intestine through effects on enteric nerves and mast cells. *Am J Physiol - Gastrointest Liver Physiol.* 1995; 269:G85–G92.
- WHO. World Malaria Report 2014. 2014.
- Wilairatana P, Meddings JB, Ho M, Vannaphan S, Looareesuwan S. Increased gastrointestinal permeability in patients with *Plasmodium falciparum* malaria. *Clin Infect Dis.* 1997; 24:430–435. [PubMed: 9114195]
- Yamatodani A, Maeyama K, Watanabe T, Wada H, Kitamura Y. Tissue distribution of histamine in a mutant mouse deficient in mast cells: clear evidence for the presence of non-mast-cell histamine. *Biochem Pharmacol.* 1982; 31:305–309. [PubMed: 7073763]
- Zabner J, Winter MC, Shasby S, Ries D, Shasby DM. Histamine decreases e-cadherin-based adhesion to increase permeability of human airway epithelium. *Chest.* 2003; 123:385S–385S. [PubMed: 12628997]

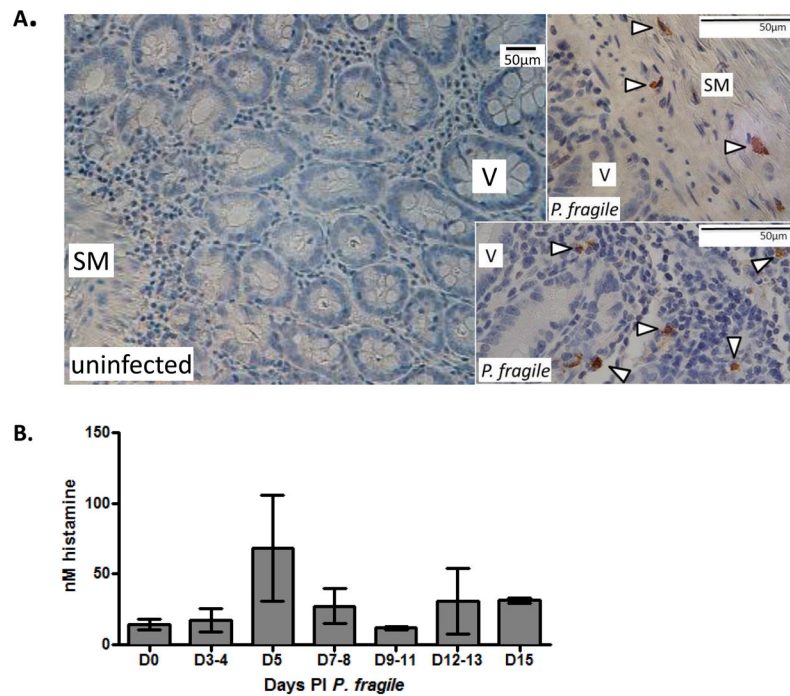


Figure 1. *Plasmodium fragile*-infected Rhesus macaques exhibit increased ileal mastocytosis and plasma histamine levels

(A) Representative ileum sections from macaques infected with *Plasmodium fragile* immunostained with anti-tryptase and counter-stained with hematoxylin. Mast cells were detected in *P. fragile*-infected animals (arrowheads, n=4) but not in uninfected controls (n=4). SM denotes submucosa, V denotes villi. Bars equal 50 μ m. (B) Mean histamine levels (\pm SEM) in plasma of *P. fragile*-infected macaques from panel A.

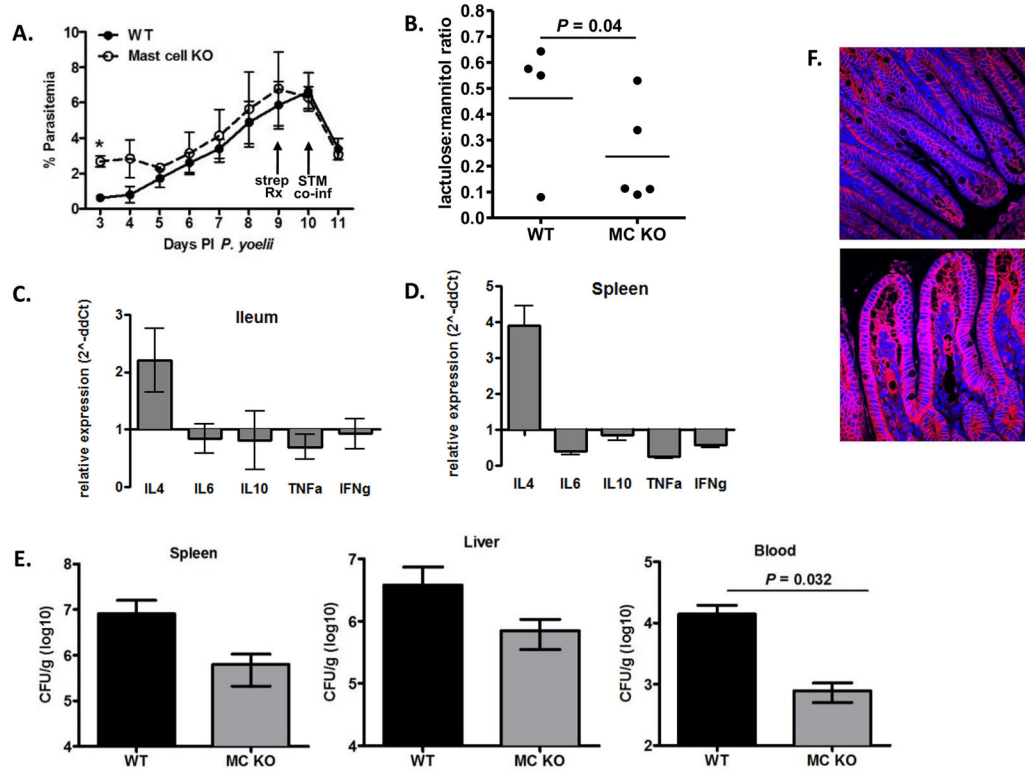


Figure 2. *Plasmodium yoelii*/S. Typhimurium co-infected mast cell deficient mice exhibit decreased intestinal permeability

Mast cell-deficient mice (n=5) and wild type controls (n=4) were infected with *P. yoelii* (day 0), orally gavaged at 9 days PI with streptomycin (strep Rx), and co-infected with *S. Typhimurium* (STM co-inf) IR715 at 10 days PI. (A) Peripheral blood parasitemias (means \pm SEM) in mice infected with *P. yoelii* at specified days PI. Mice were co-infected at 10 days PI (arrow, STM co-inf). *, $P < 0.05$ (B) Lactulose:mannitol ratios in urine from *P. yoelii*-infected mast cell-deficient mice (MC KO) and wild type (WT) controls at 1 day PI. (C, D) Fold changes in relative ileal and splenic cytokine levels ($2^{-\Delta\Delta Ct}$) in co-infected mast cell-deficient mice relative to co-infected wild type controls (set at 1) at 12 days PI *P. yoelii*/2 days post co-infection (n=4–5 mice per group). (E) Mean *S. Typhimurium* CFU/g \pm SEM in liver, spleen and blood in co-infected mast cell-deficient (MC KO) and co-infected wild type (WT) control mice at 12 days PI *P. yoelii*/2 days post co-infection (n=4–5 mice per group). (F) Representative E-cadherin (red) with DAPI nuclear (blue) stained ileum sections from co-infected WT control (top panel) and co-infected mast cell-deficient (bottom panel) mice at 12 days PI *P. yoelii*/2 days post co-infection.

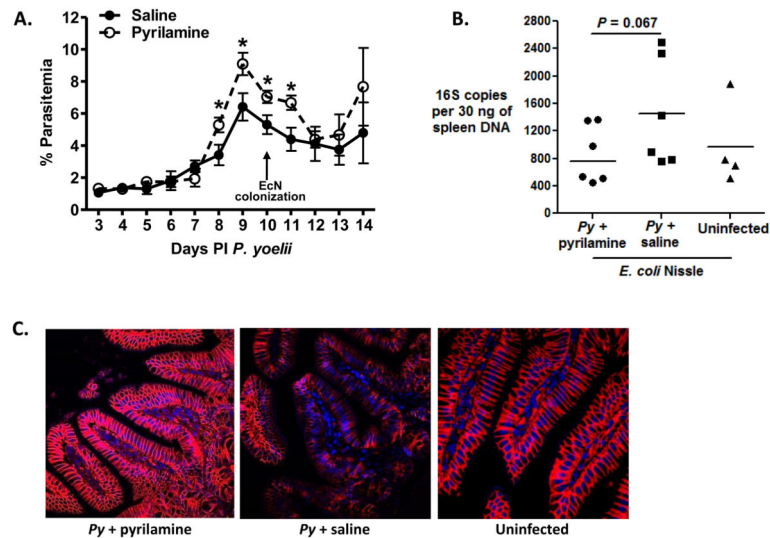


Figure 3. Antihistamine treatment during *P. yoelii* infection results in decreased intestinal permeability

P. yoelii-infected CBA/J mice were treated from days 1–8 after infection with pyrilamine or saline (vehicle control). At 10 days PI, mice were colonized with *E. coli* Nissle (EcN). Uninfected mice were colonized with EcN at 10 days after uninfected RBC inoculation. Mice were sacrificed at 14 days PI *P. yoelii*/4 days after EcN colonization for qPCR and E-cadherin immunofluorescence. (A) Peripheral blood parasitemias (means \pm SEM) in mice infected with *P. yoelii* (n=6 mice per group). Mice were colonized with EcN at 10 days PI (arrow). *, $P < 0.05$ (B) 16S rDNA copies per 30 ng spleen from pyrilamine- or saline-treated *P. yoelii*-infected mice and uninfected controls (each dot represents one mouse). (C) Representative E-cadherin (red) with DAPI nuclear (blue) stained ileum sections from pyrilamine- (left panel) and saline-treated (middle panel) *P. yoelii*-infected mice and from uninfected mice (right panel) from (B) (all EcN colonized).

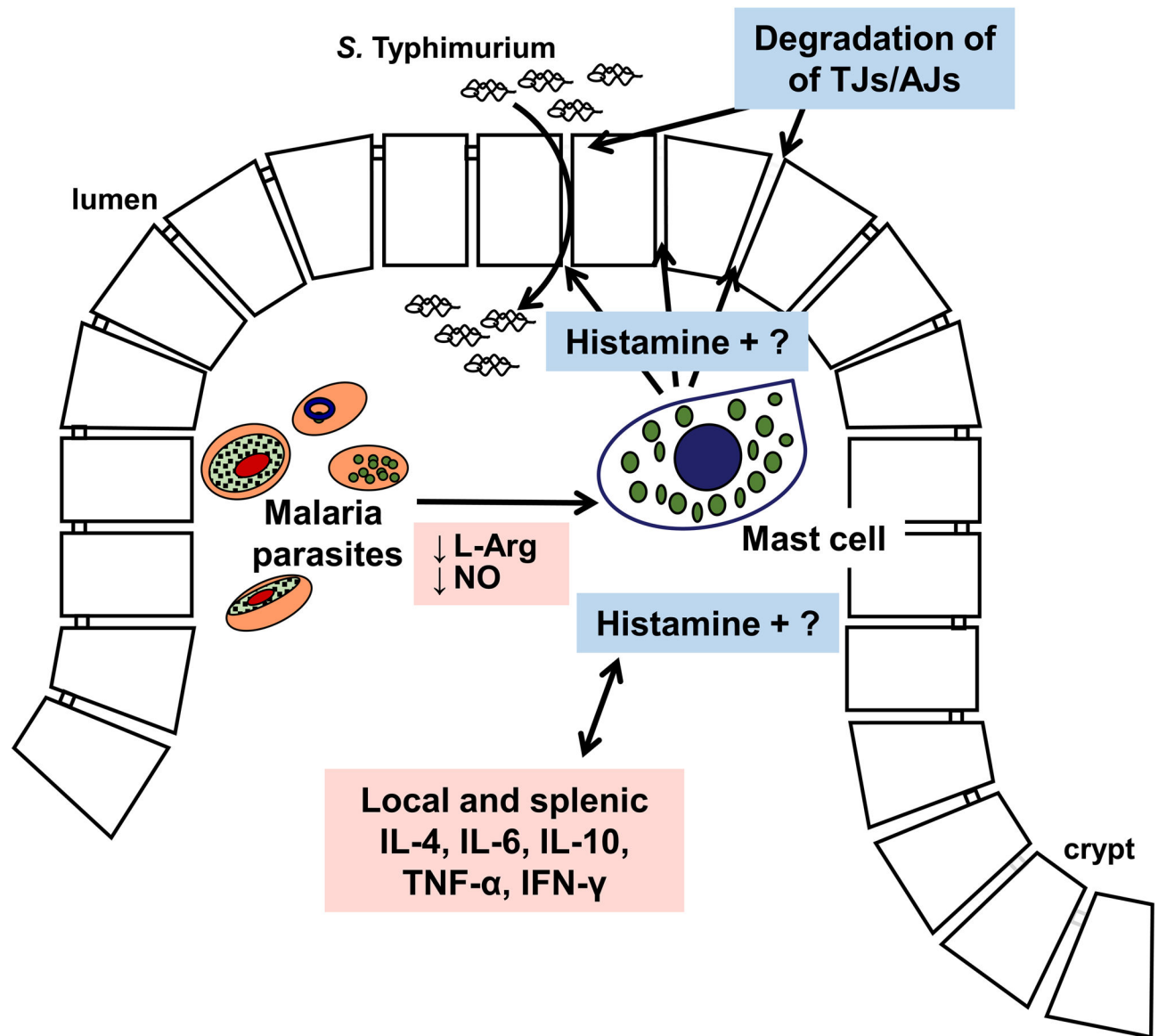


Figure 4. Mast cells and histamine alter intestinal permeability during malaria parasite infection
 Activated mast cells accumulate in highly vascularized intestinal villi following endothelial activation by low NO levels and parasite cytoadherence. Mucosal mast cell activation is sustained by low L-Arginine (L-Arg) and low NO levels in malaria as well as by cytokines that promote mast cell survival and proliferation. Activated mast cells produce a variety of factors, including histamine that can degrade the physical barrier (tight junctions, adherens junctions; TJs, AJs) to bacterial dissemination and that can crosstalk with regulatory and inflammatory cytokines (Dy and Schneider, 2004) to control multiplication of disseminated *S. Typhimurium* during co-infection (Mooney et al., 2014; Lokken et al., 2014).